

Originally published as:

Siemes, H., Rybacki, E., Kunze, K., Klingenberg, B., Naumann, M., Brokmeier, H.-G., Jansen, E. (2010):
Development of Microstructure and Texture of Hematite Ores Deformed to Large Strain in Torsion:
Can Texture Identify the Prevailing Strength and Creep Mechanisms During Deformation?. -
Advanced Engineering Materials, 12, 10, 1003-1007

DOI: 10.1002/adem.201000069

Development of microstructure and texture of hematite ores deformed to large strain in torsion: can texture identify the prevailing strength and creep mechanisms during deformation?**

By Heinrich Siemes*, Erik Rybacki, Karsten Kunze, Birgit Klingenberg, Michael Naumann, Heinz-Günter Brokmeier and Ekkehard Jansen

[*] *Prof. Dr.-Ing H. Siemes, Dipl.-Geologin B. Klingenberg*

Institut für Mineralogie und Lagerstättenlehre, RWTH Aachen

D-52056 Aachen, Germany

E-mail: siemes@rwth-aachen.de

Dr. E. Rybacki, Dipl.-Ing. M. Naumann

Geoforschungszentrum Potsdam, Deformation und Rheologie

D-14473 Potsdam, Germany

Dr. K. Kunze

Elektronenmikroskopie ETH Zürich (EMEZ)

CH-8093 Zürich, Switzerland

Prof. Dr. H.-G. Brokmeier

GKSS, Strukturforschung an Neuen Werkstoffen, Außenstelle der TU Clausthal

D-21502 Geesthacht, Germany

Dipl.-Phys. E. Jansen formerly with

Forschungszentrum Jülich, Außenstelle Mineralogisches Institut, Universität Bonn

D-52428 Jülich Germany

[**] *The authors are grateful to the DFG for financial support and the staffs of the involved institutions for their technical support. Comments by H.-R. Wenk, C. Esling and an anonymous referee are gratefully acknowledged. The Kumba Iron Ore is thanked for supplying suitable hematite ore for our experiments.*

Samples of fine-grained (~9µm) and coarse-grained (~45µm) hematite ores with almost random crystallographic preferred orientation (CPO) were deformed in high pressure, high temperature (400 MPa, 850°C-1000°C) torsion experiments up to shear strains of 4.7. Samples with large initial grain size, preferably deformed by dislocation creep attended by dynamic recrystallization, showed grain size reduction and a weak CPO (J~1.4 at 950°C). In contrast, fine-grained ores,

deformed mainly by grain boundary sliding accompanied by dislocation activity with slip on the dominant basal glide system, showed grain growth and a strong CPO ($J \sim 2.9$). At high strain both ores attained similar strength and grain size, but different CPO's. The experiments demonstrate that the texture intensity of highly deformed rocks strongly depends on initial microstructure and may not reflect unambiguously the prevailing deformation mechanism and strength as often assumed in field studies.

Hematite Fe_2O_3 is a trigonal mineral with corundum structure and the most important world wide mined iron ore. There is a long history of measurements dealing with crystallographic preferred orientation (CPO) of hematite by means of X-rays (Neff and Paulitsch, 1959^[1]) and neutron diffraction (Wagner et al. 1977^[2]). The microstructure and crystallographic preferred orientation of banded iron ores of different deposits from Brazil was objective of numerous recent publications, e.g. Rosière et al.^[3], Bascou et al.^[4], Morales et al.^[5]. The ores reveal a wide range in grain size and shape. Textural investigations show a circular to elliptical c-axis maximum centered on the pole of foliation. Poles of prism planes are aligned on great circles with a maximum centered on the lineation. The intensity of CPO, characterized by the maximum density of the c-pole figure or texture index J (Bunge^[6], Hielscher et al.^[7]) varies with the deformation history (Quade et al.^[8]; Rosière et al.^[3]), depending on metamorphic temperature ($\sim 400\text{--}600^\circ\text{C}$) and increasing strain from west to east in Quadrilátero Ferrífero (Rosière et al.^[9]), and on local intensity of shearing and folding (Morales et al.^[5]).

For the identification of the prevailing deformation mechanism in natural rocks analysis of the CPO was frequently used. A strong CPO is usually assumed to reflect dislocation creep, while low to random CPO characterizes diffusion creep. Grain boundary sliding (GBS) is considered to weaken the CPO (Mehl and Hirth^[10] and references therein). However, even for linear viscous creep a strong CPO can evolve by the evolution of a strong shape-preferred orientation at high strain (Gómez-Barreiro et al.^[11], Delle Piane et al.^[12]). Consequently, detailed knowledge of the texture intensity in response to the prevailing deformation processes is important to estimate strength at natural conditions.

Based on compression experiments on polycrystalline hematite (Siemes et al.^[13]) we performed high-strain torsion experiments to study the influence of initial microstructure and strain on the rheology and texture evolution of polycrystalline hematite. The results indicate that the starting microstructure (grain size) is an important parameter for the evolution of texture and that rock strength cannot be deduced from the CPO intensity alone.

Experimental

Starting materials were two hematite ore blocks (>98% Fe₂O₃) from the Sishen Mine, Northern Cape Province, South Africa. The ores show almost random CPO (c-axis maximum ~1.6, texture index J ~1.04) with an average grain size of ~9µm (block05) and ~45µm (block12), respectively.

Deformation experiments were performed in a HTP-torsion apparatus (Paterson and Olgaard^[14]) on cylindrical specimens of 10 mm length and 14 mm diameter. The samples were sealed by ~0.3 mm thick iron jackets from the argon confining pressure medium. In order to minimize reaction between jacket and sample forming magnetite and wuestite, the samples were encapsulated in a silver(70)/palladium(30) sleeve of 0.5 mm thickness (Siemes et al.^[13]). We performed 15 experiments in the temperature range between 800°C and 1000°C at constant shear strain rates of about $4.5 \times 10^{-5} \text{ s}^{-1}$ to finite shear strains up to $\gamma=4.7$. Maximum shear strengths τ were between 40 MPa and 95 MPa. For calculation of stress from measured torque data we assumed power law creep behavior of the form $\dot{\gamma} = A \tau^n \exp(-Q/RT)$, where n is stress exponent derived from twist-rate

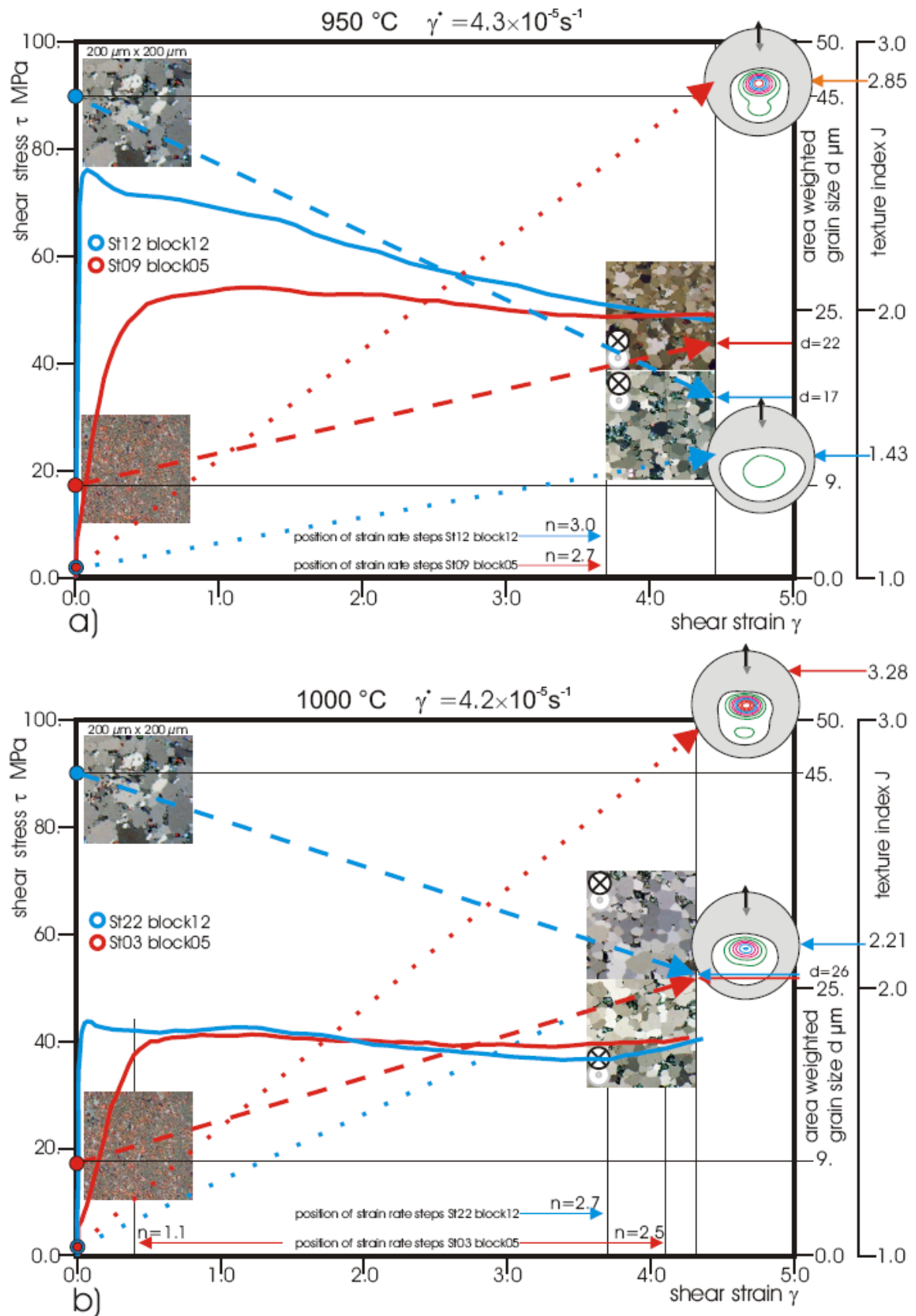


Figure 1. Shear stress-shear strain curves, microstructures, grain sizes, (0001)-pole figures, and texture indexes of torsion tests on samples of block05 and block12. a) temperature 950°C, strain rate $\dot{\gamma} = 4.3 \times 10^{-5} \text{ s}^{-1}$, finite strain $\gamma = 4.4$ b) temperature 1000°C, strain rate $\dot{\gamma} = 4.2 \times 10^{-5} \text{ s}^{-1}$, finite strain $\gamma = 4.3$.

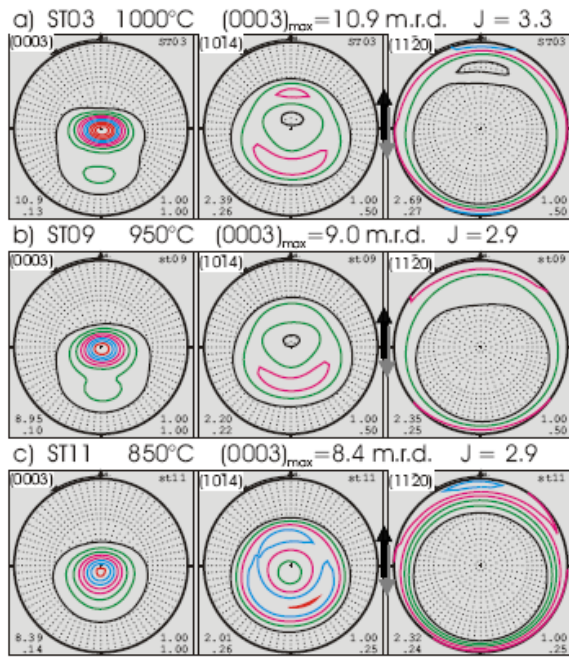


Fig. 2

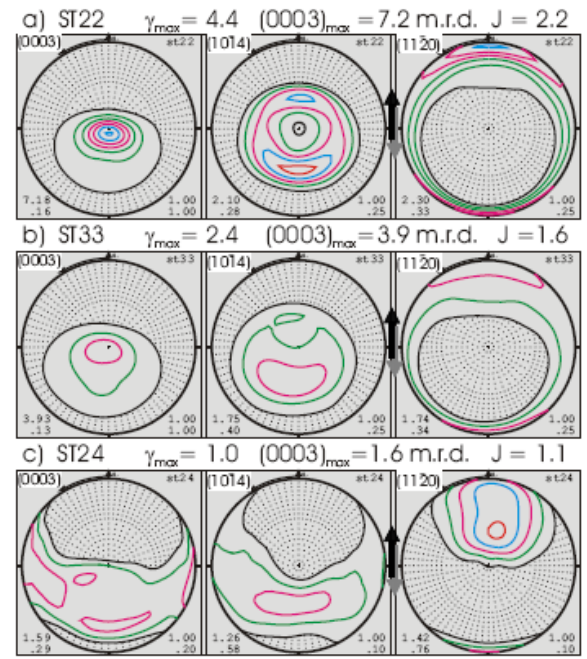


Fig. 3

Figure 2. Pole figures of three specimens (block05) deformed at 1000°C, 950 and 800°C, respectively, at the same strain rate $\dot{\gamma} \sim 4.3$ to the same final strain $\gamma \sim 4.4$

All pole figures are equal area projections parallel to the shear plane. The shear direction is specified by black arrows. In the lower left corner of the figures are indicated the maximum and minimum densities, in the lower right corner the first contour line and the contour intervals. The dotted area is below 1.0 m.r.d. (multiples of random density).

Figure 3. Pole figures of three specimens (block12) deformed at 1000°C, a strain rate of $\dot{\gamma} \sim 4.3 \times 10^{-5} \text{ s}^{-1}$ to different final strains $\gamma = 4.4$, $\gamma = 2.4$ and, $\gamma = 1.0$, respectively. Explanation of pole figures are given in figure caption of Fig. 2.

stepping tests, Q is activation energy derived from temperature stepping tests, and τ is derived from torque data according to Paterson and Olgaard^[14]. Calculated stress-strain data were corrected for system compliance and strength of metal jackets.

Grain size was measured on optical microphotographs. Individual grain boundaries were manually traced and subsequently analyzed with the ImageJ v1.36 software (Rusband^[15]). As a proxy for grain size we used the area weighted grain size (see Ebert et al.^[16] and discussion therein).

To determine the CPO we used neutron diffraction texture analysis (FZ Jülich: Jansen et al.^[17] and GKSS Geesthacht: Brokmeier et al.^[18]) with data processing using MTEX (Hielscher and Schaeben^[19]) and EBSD-measurements (Kunze et al.^[20,21]). For neutron diffraction we prepared

prismatic samples of $2 \times 2 \times 10 \text{ mm}^3$ at the periphery and oriented parallel to the axis of deformed samples.

Results

Typical strain stress curves of highly deformed hematite are illustrated in Figure 1 for temperatures of 950° and 1000°C and $\dot{\gamma} \approx 4.3 \times 10^{-5} \text{ s}^{-1}$. At 950°C the initially coarse-grained hematite (block12) shows strain weakening until $\gamma \sim 4.4$ where stress is equal to the quasi steady state strength of the initially fine-grained hematite (block05) (Figure 1a). At $T = 1000^\circ\text{C}$ both ores exhibit nearly equal steady state behavior (Figure 1b). At both temperatures the fine-grained samples reach the maximum stress at a $\gamma \approx 0.5$ and the coarse-grained rocks at $\gamma \approx 0.1$. From strain rate-stepping tests (Paterson and Olgaard ^[14]) we obtained a stress exponent of $n = 3.0\text{-}2.7$ for the coarse-grained hematite and $n = 2.7\text{-}2.5$ for the fine-grained hematite with lower values obtained at higher temperature.

The final grain size is quite similar at given experimental conditions, irrespective of the initial grain size. It decreases with increasing stress and decreasing temperature, respectively. However, at both temperatures the final texture of fine-grained samples is considerably stronger than of coarse-grained hematite as shown for the basal (0001)-pole figures in Figure 1. The basal (0001)-pole figures show elliptical maxima close to the shear plane normal and the prism planes develop great circle distributions with a maximum centered on the shear direction. For a given starting microstructure the intensity of CPO increases slightly with increasing temperature from 850° to 1000°C (Figure 2) and strongly with increasing strain from 1 to 4.4 (Figure 3). The {10-14}-pole figures with two banana-like maxima (Quade^[22]) are presented for comparison with the preferentially measured {10-14}-pole figures by X-rays.

To determine the texture dependence on strain we additionally analyzed one coarse-grained sample deformed at 950°C with EBSD-mapping (Kunze et al.^[21]) of a cross-section from the center towards the circumference, for which shear strain increases linearly and stress non-linearly from inward to outward. The sample shows a continuous decrease of grain size from 28 to 22 μm and a continuous increase of CPO intensity from $J=1.3$ to $J=2.1$ up to $\gamma \approx 3.2$, beyond which changes are minor (Figure 4). The final texture index J obtained from neutron-diffraction is about 1.5, owing to the larger volume analyzed compared to EBSD surface measurements. The small grain size measured close to the sample center shows that grain size reduction already occurs at very low strain. The experimentally derived textures and microstructures agree well with the textures and granoblastic microstructures of naturally deformed ores.



Figure 4. Orientation mapping of central cut through torsion sample ST27 block 12, 950°C, $\dot{\gamma} = 4.7 \times 10^{-5} \text{ s}^{-1}$, $\gamma = 4.7$. Color key according to IPF for torsion axis (normal to shear plane). An average gradient of crystal preferred orientation ($J=1.3 \rightarrow J=2.1$, white line) and in grain size area ($28 \mu\text{m} \rightarrow 22 \mu\text{m}$, yellow line) evolved from inside to outside of the torsion cylinder.

Discussion

Indicative for the rate-limiting deformation process is the magnitude of the stress exponent n . An exponent of $n=1$ indicates predominantly diffusion processes, $n \geq 3$ dislocation glide and climb (creep), and $n=2$ dislocation-accommodated grain boundary sliding (e.g. discussion in Gómez-Barreiro et al.^[11]). The measured range of n and the isometric final grain shape suggests that the hematite was deformed by a combination of intracrystalline dislocation creep and grain boundary sliding (GBS).

Intuitively one would expect that the contribution of GBS in comparison to dislocation creep is larger for deformation of samples with initially small grain size than for coarse-grained rocks. If strain during dislocation creep is dominantly accommodated by glide on the easiest slip system (e.g. basal glide of hexagonal crystals) and with ongoing deformation grains rotate toward orientations that promote slip on the dominant slip system (see figs. 8 and 10 in Beausir et al.^[23]), a strong texture evolution is expected. Therefore, coarse-grained rocks should exhibit stronger CPO than fine-grained starting materials, since grain boundary sliding is supposed to reduce texture strength (Gómez-Barreiro et al.^[11] and references therein). However, the texture of deformed hematite with initially fine grains is much stronger than of initially coarse-grained hematite, even when deformed to similar strain under similar conditions and with initially random CPO. Presumably a rather complex interaction and competition of dislocation creep, grain boundary sliding, dynamic recrystallization, and grain growth is responsible for the different deformation behavior and texture evolution of the two ores.

At $T = 950^\circ\text{C}$ the coarse-grained ore requires a high peak stress ($\sim 76 \text{ MPa}$) to initiate plastic deformation in the dislocation creep regime by multiple slip (v. Mises^[24] criterion) that should increase the CPO. With ongoing deformation dynamic recrystallization to smaller grain sizes occurs (Figures 1,4). It is assumed that the CPO of the new nucleated grains is weaker than that of the bulk

sample (e.g. Lee et al.^[25]). Reducing the grain size also promotes GBS and reduces shear stress since GBS is grain size dependent (Nieh et al.^[26]). This results in a competition between increasing CPO by slip and rotation of grains into the position with (0001) parallel to the shear plane and lowering the CPO by recrystallization and GBS. The weak final texture ($J \sim 1.4$) suggests that the latter processes are more effective. EBSD mapping (Figure 4) shows that once grain refinement by recrystallization reached a steady-state size, also the texture index J remains nearly constant, i.e. the competition of the different deformation and recovery processes reached an equilibrium that is also reflected associated in almost constant strength. In contrast, the fine-grained ore yields at low stresses (~ 7 MPa) and inelastic deformation presumably continues preferentially GBS accommodated by single slip on the dominant basal glide system (0001) $\langle 11\bar{2}0 \rangle$ at relaxed v. Mises condition (Lee et al.^[25], Drury and Fitz Gerald^[27]). With ongoing deformation grain growth to a steady state grain size (Shimizu^[28]) occurs combined with slip, which may additionally promote the development of preferred orientation. A strong texture ($J=2.9$) evolves by rotation of (0001) parallel to the shear plane and prism planes normal to the shearing direction.

For samples deformed at 1000°C the shear stress (40 MPa) is lower than at 950°C because the critical resolved shear stresses of the glide systems decrease with increasing temperature (Siemes et al.^[29]). Again, the texture index for the specimen of the fine-grained block05 is higher ($J=3.3$) than for the coarse-grained block12 ($J=2.2$). The difference is much smaller than at 950°C, presumably because both samples deformed by the same deformation mechanisms over a large strain interval as verified by the similarity of stress-strain curves.

With increasing temperature the texture index J increases slightly for the fine-grained starting material, probably because of enhanced grain growth at high temperature, which promotes deformation accompanied by slip and therefore increased CPO. The shape of the stress-strain curves suggest that grain growth to an equilibrium grain size with stress is reached at a strain of about 0.5. For the coarse-grained hematite the texture index is also higher after deformation at 1000°C than at 950°C, but the difference is more pronounced than for the fine-grained material. This is probably linked to strain weakening at low T associated with continuous recrystallization and a weaker increase of CPO than for the fine-grained rocks, for which stress is constant after yielding. Since the equilibrium grain size is smaller at high stress (low temperature), more intense recrystallization is required that also reduces the CPO.

Conclusions

Based on high strain torsion experiments on hematite with initially random CPO but different grain size, we demonstrated that the evolution of a strong CPO is not unambiguously associated with high strength. Instead, the relative contributions of dislocation creep and grain boundary sliding, associated with dynamic recrystallization and grain growth determines the final CPO after

deformation. The CPO can easily differ up a factor of 2 (at 950°C and possibly more at lower T) for rocks that were highly deformed even under similar stress, but with different starting microstructure.

- [1] H. Neff, P. Paulitsch. Bestimmung natürlicher Korngefüge mit dem Zählrohrgoniometer. *Naturwissenschaften* **1959**, 46, 490.
- [2] F. Wagner, C. Esling, R. Baro, M. Englander. Textures of iron oxide ores by neutron diffraction and topotactical relation. *International Journal of Materials Research (Zeitschrift für Metallkunde)* **1977**, 68, 701-705.
- [3] C.A. Rosière, H. Siemes, H. Quade, H.-G. Brokmeier, E.M. Jansen. Microstructures, textures and deformation mechanisms in hematite. *Journal of Structural Geology* **2001**, 23, 1429-1440.
- [4] J. Bascou, M.I.B. Raposo, A. Vauchez, M. Egydio-Silva. Titanohematite lattice-preferred orientation and magnetic anisotropy in high-temperature mylonites. *Earth and Planetary Science Letters* **2002**, 198, 77-92.
- [5] L.F.G. Morales, L.E. Lagoeiro, I. Endo. Crystallographic fabric development along a folded polycrystalline hematite. *Journal of Structural Geology* **2008**, 30, 1218-1228.
- [6] H.J. Bunge, *Texture Analysis in Materials Science*, Butterworths London, **1982**, English
Translation of *Mathematische Methoden der Texturanalyse*, Akademie Verlag Berlin, **1969**.
- [7] R. Hielscher, H. Schaeben, D. Chateigner. On the entropy to texture index relationship in quantitative texture analysis. *Journal Applied Crystallography* **2007**, 40, 371-365.
- [8] H. Quade, C.A. Rosière, H. Siemes, H.-G. Brokmeier, Fabrics and textures of Precambrian iron ores from Brazilian Deposits. *Zeitschrift für angewandte Geowissenschaften*, **2000**, SH1, 155-162.
- [9] C.A. Rosière, C.A. Spier, F.J. Rios, V.E. Suckau. The Itabirites of the Quadrilátero Ferrífero and related high-grade iron ore deposits: an overview. In: Banded Iron Formation–Related High-Grade Iron Ore (Eds: S. Hagemann, C.A. Rosière, J. Gutzmer, N. Beukes), *Reviews in Economic Geology* **2008**, 15, 223-254.
- [10] L. Mehl, G. Hirth. Plagioclase preferred orientation in layered mylonites: Evaluation of flow laws for the lower crust. *Journal of Geophysical Research* **2008**, 113, B05202.
- [11] J. Gómez-Barreiro, I. Leonardelli, H.-R. Wenk, G. Dresen, E. Rybacki, Y. Ren, C.N. Tomé. Preferred orientation of anorthite deformed experimentally in Newtonian creep. *Earth and Planetary Science Letters* **2007**, 264, 188-207.
- [12] C. Delle Piane, L. Burlini, K. Kunze. The influence of dolomite on the plastic flow of calcite. Rheological, microstructural and chemical evolution during large strain torsion experiments. *Tectonophysics* 2009, **467**, 145-166. doi:[10.1016/j.tecto.2008.12.022](https://doi.org/10.1016/j.tecto.2008.12.022)

- [13] H. Siemes, B. Klingenberg, E. Rybacki, M. Naumann, W. Schäfer, E. Jansen, C.A. Rosière. Texture, microstructure, and strength of hematite ores experimentally deformed in the temperature range 600-1100°C and at strain rates between 10^{-4} and 10^{-6} s⁻¹. *Journal of Structural Geology* **2003**, 25, 1371-1391.
- [14] M.S. Paterson, D.L. Olgaard. Rock deformation tests to large shear strains in torsion. *Journal of Structural Geology* **2000**, 22, 1341-1358.
- [15] W.J. Rusband. ImageJ, U.S. National Institute of Health (NIH) **2006**. <http://rsb.info.nih.gov/ij/>.
- [16] A. Ebert, M. Herwegh, B. Evans, A. Pfiffner, N. Austin, T. Vennemann. Microfabrics in carbonate mylonites along a large-scale shear zone (Helvetic Alps). *Tectonophysics* **2008**, 444, 1-26
- [17] E. Jansen, W. Schäfer, A. Kirfel. The Jülich neutron diffractometer and data processing in rock texture processing. *Journal of Structural Geology* **2000**, 22, 1559-1564.
- [18] H.G. Brokmeier, U. Zink, R. Schnieber, B. Witassek. TEX-2, texture analysis at GKSS Research Center (instrumentation and application). *Materials Science Forum* **1998**, 273-275, 277-282.
- [19] R. Hielscher, H. Schaeben. A novel pole figure inversion method: specification of the MTEX algorithm. *Journal of Applied Crystallography* **2008**, 41, 1024-1037.
- [20] K. Kunze, S.I. Wright, B.L. Adams, D.J. Dingley. Advances in automatic EBSD single orientation measurements. *Textures and Microstructures* **1993**, 20, 51-54.
- [21] K. Kunze, H. Siemes, E. Rybacki, E. Jansen, H.-G. Brokmeier. Microstructure and texture from experimentally deformed hematite ore. In: *EMC 2008, Vol.2: Materials Science, 14th European Microscopy Congress* (Eds: S. Richter, A. Schwedt) Springer-Verlag **2008**, 827-828.
- [22] H. Quade. Natural and simulated (10.4) pole figures of polycrystalline hematite. *Textures and Microstructures* **1998**, 8-9, 719-736.
- [23] B. Beausir, L.S. Toth, K.W. Neale. Ideal orientations and persistence characteristics of hexagonal close packed crystals in simple shear. *Acta Materialia* **2007**, 55, 2695-2705.
- [24] R. von Mises. Mechanik der plastischen Formänderung von Kristallen. *Zeitschrift für angewandte Mathematik und Mechanik* **1928**, 8, 161-185.
- [25] K.H. Lee, Z. Jiang, S.I. Karato. A scanning microscope study of the effects of dynamic recrystallization on lattice preferred orientation in olivine. *Tectonophysics* **2002**, 351, 331-341.
- [26] T.G. Nieh, J. Wadsworth, O.D. Sherby. *Superplasticity in Metals and Ceramics*. Cambridge University Press **1997**, pp 273.
- [27] M.R. Drury, J.D. Fitz Gerald. Mantle rheology: insights from laboratory studies of deformation and phase transition. In: *The Earth's Mantle* (Ed. I. Jackson), Cambridge University Press **1998**, 503-559.
- [28] I. Shimizu. Theories and applicability of grain size piezometers: The role of dynamic recrystallization mechanisms. *Journal of Structural Geology* **2008**, 30, 899-917.

- [29] H. Siemes, B. Klingenberg, E. Rybacki, M. Naumann, W. Schäfer, E. Jansen, K. Kunze. Glide systems of hematite single crystals in deformation experiments. *Ore Geology Reviews* **2008**, 33, 255-279.